Cryptorchidism in the Orl Rat Is Associated with Muscle Patterning Defects in the Fetal Gubernaculum and Altered Hormonal Signaling[1]

Julia S. Barthold,[2,3] Alan Robbins,[3] Yanping Wang,[3] Joan Pugarelli,[3] Abigail Mateson,[3] Ravinder Anand-Ivell,[4] Richard Ivell,[5] Suzanne M. McCahan,[3] and Robert E. Akins, Jr[3]

[3]Nemours Biomedical Research/Alfred I. duPont Hospital for Children, Wilmington, Delaware
[4]Division of Animal Sciences, University of Nottingham, Leicestershire, United Kingdom
[5]Leibniz Institute for Farm Animal Biology, Dummerstorf, Germany

ABSTRACT

Cryptorchidism, or undescended testis, is a common male genital anomaly of unclear etiology. Hormonal stimulation of the developing fetal gubernaculum by testicular androgens and insulin-like 3 (INSL3) is required for testicular descent. In studies of the orl fetal rat, one of several reported strains with inherited cryptorchidism, we studied hormone levels, gene expression in intact and hormone-stimulated gubernaculum, and imaging of the developing cremaster muscle facilitated by a tissue clearing protocol to further characterize development of the orl gubernaculum. Abnormal localization of the inverted gubernaculum was visible soon after birth. In the orl fetus, testicular testosterone, gubernacular androgen-responsive transcript levels, and muscle-specific gene expression were reduced. However, the in vitro transcriptional response of the orl gubernaculum to androgen was largely comparable to wild type (wt). In contrast, increases in serum INSL3, gubernacular INSL3-responsive transcript levels, expression of the INSL3 receptor, *Rxfp2,* and the response of the orl gubernaculum to INSL3 in vitro all suggest enhanced activation of INSL3/RXFP2 signaling in the orl rat. However, DNA sequence analysis did not identify functional variants in orl *Insl3*. Finally, combined analysis of the present and previous studies of the orl transcriptome confirmed altered expression of muscle and cellular motility genes, and whole mount imaging revealed aberrant muscle pattern formation in the orl fetal gubernaculum. The nature and prevalence of developmental muscle defects in the orl gubernaculum are consistent with the cryptorchid phenotype in this strain. These data suggest impaired androgen and enhanced INSL3 signaling in the orl fetus accompanied by defective cremaster muscle development.

androgen receptor, cryptorchidism, gubernaculum, insulin-like 3, male reproductive tract

INTRODUCTION

Testicular descent is a complex process that requires the gubernaculum, a specialized intermediate mesoderm derivative that is developmentally responsive to stimulation by the Leydig cell hormones insulin-like 3 (INSL3) and androgen. These hormones target their receptors, the relaxin-insulin-like family peptide receptor 2 (RXFP2) and androgen receptor (AR), respectively, in the developing rat fetal gubernaculum during a swelling phase that occurs between Embryonic Days 16 and 19 (E16 and E19). The cremaster muscle develops within the periphery of the enlarging fetal gubernaculum, together called the gubernaculum/cremaster complex, which inverts around the time of birth (E22) to form a muscular sac into which the testis descends. Transplacental exposure to antiandrogens between E16 and E19, but not later, inhibits both gubernacular enlargement and testicular descent in the fetal rat [1–3]. In man and larger mammals, the cremaster muscle develops within a longer inguinal canal, and muscle fibers extend into the developing mesenchymal core [4]. Abundant production of proteoglycans (PG) occurs within this core and the hydration associated with PG production contributes to a prominent swelling reaction just prior to testicular descent [5].

Targeted disruption of either *Ar* (the GU-ARKO mouse) [6] or *Rxfp2* [7] in the gubernacular mesenchyme, but not in committed muscle cells, results in impaired testicular descent; however, cryptorchid and gubernacular developmental phenotypes are more severe for *Rxfp2*. In the *Rxfp2* knockdown model, there is failure of enlargement, disorganization of the peripheral cremaster muscle layer, ectopic localization of muscle cells within the central mesenchymal core, and failure of AR$^+$ cells fail to migrate into the developing gubernaculum [7]. In contrast, formation of the cremasteric sac still occurs in GU-ARKO mice, but muscle organization and growth are impaired while expression of muscle-specific markers is altered in the postnatal cremaster and testicular descent fails to occur [6]. The swelling reaction of the gubernaculum is less conspicuous in rodents than in larger mammals but is absent or blunted with targeted deletion of hormone receptors in undifferentiated gubernacular cells. Therefore, both hormonal pathways facilitate testicular descent by regulating the muscle development and extracellular matrix (ECM) production that contribute to swelling of the developing gubernaculum.

Gene expression profiling following in vitro exposure of the rat gubernaculum to INSL3 or dihydrotestosterone (DHT) at E17 revealed strong overlap in altered transcript levels, most notably those involved in Wnt signaling [8, 9]. Knowledge of hormone-responsive transcripts in wild-type (wt) Long Evans (LE) gubernacula has provided a basis for comparative expression profiling in the orl rat strain, a closed LE-derived rat colony with spontaneous, inherited cryptorchidism. Micro-dissection [10] and gene expression [11] studies of the perinatal

orl gubernaculum show mild phenotypic abnormalities, including dysmorphic prenatal appearance with significant elongation and thinning and delayed inversion at birth, and altered expression of muscle- and cytoskeleton-specific transcripts. About 60% of orl males are cryptorchid with testes in the superficial inguinal pouch, and the phenotype is unilateral in the about 75% of cases; therefore, approximately half of testes migrate into an aberrant position. Genome mapping shows association of the cryptorchid orl phenotype with multiple loci, and selective breeding confirmed that enrichment of potential risk alleles on chromosomes 6 and 16 can recapitulate the phenotype in crossbred wt strains (Barthold et al., unpublished results). Therefore, orl cryptorchidism is inherited as a complex, multilocus trait with reduced penetrance and with a gubernacular phenotype that is mild compared to the $Rxfp2^{-/-}$ mouse. Molecular phenotyping may help to validate candidate risk alleles and define the genetic basis of cryptorchidism in this strain.

The present studies were designed to provide additional insight into testicular hormone production and response in the orl strain and to complement ongoing efforts to characterize the genetic basis of cryptorchidism in this isolated rat colony. Our data suggest increased activation of INSL3-RXFP2 signaling but reduced androgen production and transcriptional response in the intact orl fetus. The present results also confirm previous studies showing altered muscle-specific transcript expression in the developing gubernaculum, and three-dimensional imaging provides further evidence for muscle patterning defects in the orl fetal gubernaculum. In combination with ongoing genetic studies, these data will help to elucidate the molecular basis of cryptorchidism in a phenotypically relevant animal model.

MATERIALS AND METHODS

Animals

All the rats were maintained at the Nemours Biomedical Research facility, which is accredited by the Association for Assessment and Accreditation of Laboratory Animal Care International, and animal care and use was approved by the Institutional Animal Care and Use Committee. Rats received food (Lab Diet Rat Chow 5021; PMI Nutrition International) and water ad libitum and were housed in polycarbonate cages with pine shaving bedding in a room with a 12L:12D cycle and controlled temperature (68°C ± 2°C) and humidity (35%–70%). The orl colony is continuously bred at our institution, and wt Long-Evans (LE) and Sprague Dawley (SD) strains were obtained from Charles River Laboratories. Because LE is the orl parent strain, it was used as a comparison strain for all the experiments that utilized orl tissues and is referred to as wt throughout the manuscript. Charles River Laboratories rats were allowed an adjustment period after transport prior to generation of timed pregnancies. Vaginal smears were used to document the presence of sperm, and the morning of the day of detection was designated E0. Necropsies were performed between 1200 and 1500 h at defined time points from E17 and Postnatal Day 35 (P35) with the day of birth defined as P0. Dams and postnatal males were euthanized by carbon dioxide asphyxiation, followed by decapitation of fetuses and neonates. The inguinoscrotal region of euthanized postnatal males was visualized using a stereoscopic, zoom, dissecting microscope, and in preliminary studies, the extent of cremaster sac migration was visualized using intraperitoneal injection of diluted, nonfluorescent dye. For mRNA analysis, direct visualization alone was used to isolate and dissect cremaster sac samples.

Serum and Tissue Sample Preparation

Euthanized fetuses were sexed, maintained on ice, and rapidly dissected in individual sterile dishes to collect blood via capillary tubes after aortic transection. Testes, gubernacula, or cremaster sacs were harvested at E17, E19, E21, P3, or P30 as indicated and frozen at −70°C in Qiagen RLT buffer. Total RNA was isolated using the RNeasy Micro kit (Qiagen) and was treated with DNAase type 1.

Serum INSL3 Measurements

Serum INSL3 was measured using a previously described time-resolved fluorescence immunoassay platform [12]. Sample volumes of 50 μl were used throughout. Standard curves were generated using concentrations ranging from 20 pg to 20 ng rat INSL3 per ml.

Isolation of Genomic DNA and Sequencing

Genomic DNA was isolated using ArchivePure Tissue extraction kits (5 Prime) following the manufacturer's protocol. Polymerase chain reaction (PCR) was used to amplify genomic DNA in the INSL3 promoter region and in a region spanning both exons and the 5′ and 3′ untranslated regions (UTR). Oligonucleotide primers were: promoter/forward: GCTCCTGGCA CAGTGCTGCAC, reverse: CAGCTGTGTAAAGGGCTTCACTC; intragenic/forward: GCATGCAGTCCTTGGCTCGCC, reverse: GACCACAGA GCTTGGCGCGCG. PCR was carried out using Titanium taq DNA polymerase (Clontech) and standard amplification protocols. PCR products were analyzed on a 1% agarose/1X TAE buffer (40 mM tris-acetate and 1 mM ethylenediaminetetraacetic acid, pH 8.0) gel. Following gel analysis, an aliquot of the PCR product was treated with Exosap (U.S. Biochemicals), and the PCR products were submitted for DNA sequencing using the BigDye Terminator v3.1 Cycle Sequencing Kit and appropriate primers. Sequencing reactions were purified to remove residual dye using Performa DTR Gel Filtration Cartridges. Subsequently samples were submitted for sequence analysis on an Applied Biosystems 3130X genetic analyzer. Sequence data were analyzed using Vector NTI Software (Life Technologies) and compared with those deposited in Variant Visualizer (http://rgd.mcw.edu/) [13].

Real-Time Quantitative Reverse Transcription Polymerase Chain Reaction

Total RNA purification, cDNA generation, TaqMan-based quantitative reverse transcription-PCR (qRT-PCR), and data analysis using the ddCT method were performed as described previously [8, 9]. Genes of interest were analyzed as in previous studies using freshly isolated wt and orl gubernaculum and testis samples, or orl gubernacula that were cultured for 24 h with INSL3 (0, 0.1, 1, 10, and 100 nM) or DHT (0, 30, or 100 nM) following a 24-h washout period (n = 5–20 replicates/group from ≥2 litters). Expression of target genes was normalized to $Gapdh$ expression and quantified relative to expression, when measureable, in a fetal rat embryo total RNA preparation (Applied Biosystems/Ambion). We used the following prevalidated TaqMan gene expression assays (Applied Biosystems): $Adh1$: Rn00570670_m1; Ar: Rn00560747_m1; $Bmp3$: Rn00567346_m1; $Bmp4$: Rn00432087_m1; $Chrdl2$: Rn01510694_m1; $Crlf1$: Rn01419973_m1; $Cxcl12$: Rn00573260_m1; $Gapdh$: Rn99999916_s1; $Has2$: Rn00565774_m1; $Myh3$:Rn00561539_m1; $Myh7$: Rn00568328_m1; $Myog$: Rn00567418_m1; $Nptx2$, Rn01756377_m1; Npy: Rn01410145_m1; $Pnoc$: Rn00564560_m1; $Sfrp2$: Rn01458837_m1; $Slit3$: Rn00580013_m1; $Tgfb2$: Rn00579674_m1; $Wnt4$: Rn00584577_m1; and $Wnt5a$: Rn00575260_m1.

Microarrays

LE (wt) and orl gubernacular RNA harvested at E17 or E19 (n = 7 per group except for wt E17, where n = 5) were used for hybridization to Affymetrix arrays as described previously [8, 9, 11]. Briefly, total RNA was labeled using the GeneChip 3′ IVT Express Kit (Affymetrix Inc.) and biotin-labeled cRNA was hybridized to GeneChip Rat Genome 230 2.0 Affymetrix arrays. Raw signal intensities for each probe set were background corrected, normalized, and summarized using GC Robust Multiarray Analysis (GC-RMA) and the afflmGUI Bioconductor package within R [14]. Array data are deposited in GEO (Gene Expression Omnibus of the National Center for Biotechnology Information; www.ncbi.nlm.nih.gov/geo/, accession numbers GSE19658 and GSE57924).

Bioinformatics and Statistical Analysis

Analysis of the microarray data was performed as previously reported [8, 11, 14] with some modification in the functional analysis of probe set lists. Briefly, after filtering low expression probe sets, we used the LIMMA package in Bioconductor and a linear model approach with false discovery rate correction to identify differentially expressed probe sets in strain (wt vs. orl) and gestational day (E17 vs. E19) comparisons (q-value < 0.05) [15]. Analysis of the following lists was performed: (a) probe sets with significant expression changes between E17 and E19 in wt males, (b) all probe sets with significant expression changes between wt and orl at E17 and/or E19, and (c) differentially
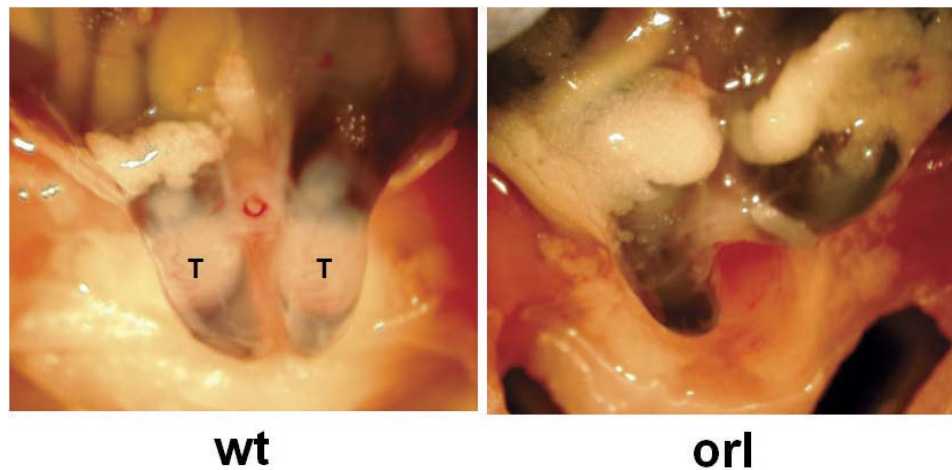
FIG. 1. Cremaster sac inversion as visualized by intraperitoneal dye injection. By Postnatal Day 3 (P3), inversion has occurred in both wt (left) and orl (right) pups. Sacs contain testes (T) in wt males at this age, and although not extending the full length of the perineum, they are well-developed. In orl pups, sacs are empty, and in this example, the left sac has inverted laterally, toward the superficial inguinal pouch, the location of cryptorchid testes in orl males. Original magnification ×7.5.

expressed probe sets in wt versus orl comparisons with fold-change differences greater than or equal to an absolute value of 1.5 or 2.0. We used Ingenuity Pathway Analysis (IPA) (Ingenuity Systems, www.ingenuity.com) to map the probe set lists to genes and to identify significantly overrepresented functional annotations and canonical pathways enriched in each list, and used multiple testing correction (a Benjamini-Hochberg-corrected Fisher exact test P value of less than 0.05) to define statistical significance. We also compared these IPA-derived lists with those previously generated in microarray experiments of fetal gubernaculum following exposure to (a) 10 or 100 nM INSL3 [9] or (b) 30 or 100 nM DHT [8] in vitro. Quantitative RT-PCR data were analyzed after log transformation with IBM SPSS Statistics v. 22 using one-way ANOVA with least significant difference post hoc testing or univariate two-way ANOVA (UNIANOVA), and P values < 0.05 were considered significant.

Antibody Labeling and Imaging

In order to visualize the three-dimensional architecture of the cremaster muscle within the fetal gubernaculum just prior to inversion, we developed a whole mount protocol that utilizes tissue clearing and immunostaining with labeled A4.1025, a myosin-specific antibody. A4.1025 hybridoma cells (Developmental Studies Hybridoma Bank) were recovered and grown in culture according to established Developmental Studies Hybridoma Bank protocols. At maturity, supernatant was collected, filtered (0.2 μm), and preserved with 0.02% sodium azide. Supernatant was purified with Protein G-conjugated beads using recommended purification buffers (Invitrogen) but with a modification of the manufacturer's protocol. Immunoglobulin was concentrated, and serum albumin was removed from the supernatant by ultrafiltration through 100 000 MWCO filters (Millipore) five times at 4000 × g for 30 min and then resuspended in PBS. The partially purified and concentrated supernatant was suspended in 30 ml of equilibration buffer (0.01 M sodium phosphate [pH 7.0], 0.15 M sodium chloride), filtered, mixed with 2 ml of protein G beads, and incubated overnight at 4°C with shaking. The mixture was filtered, and beads were washed in equilibration buffer and eluted. Aliquots were brought to pH 7.4, and the protein concentration was determined with a Qubit Fluorometer (Life Technologies). Protein-containing aliquots were desalted via 10 000 MWCO ultrafiltration, centrifuged four times at 4000 × g for 30 min, then resuspended in PBS and brought to a standard protein concentration of 1 mg/ml. Concentrated A4.1025 antibody was directly labeled using the AlexaFluor 555 Antibody Labeling Kit (A20187; Life Technologies) according to the manufacturer's directions. Antibody specificity for myosin heavy chain was confirmed using rat heart muscle and skeletal muscle sections.

Gubernacula were dissected from E21 pups and immediately fixed in freshly prepared 4% paraformaldehyde PBS at 4°C overnight. After removal from 4% paraformaldehyde PBS, gubernacula were rinsed and incubated for 1 h on ice in 100% methanol and then stored at −20°C. A published benzyl alcohol:benzyl benzoate protocol was used for tissue clearing [16]. Briefly, gubernacula were placed in Dent bleach (methanol:dimethylsulfoxide:H_2O_2, 4:1:1) [17] for 2 h at room temperature and then rehydrated through a series of decreasing methanol concentrations in PBS with 0.1% Tween 20. The samples

were then blocked in TNB buffer (Perkin-Elmer) in PBS for 2 h. Gubernacula were incubated overnight with 1:500 labeled A4.1025 anti-myosin antibody in 0.5% TNB/PBS at 4°C with gentle agitation, then washed five times for 1 h with PBS with 0.1% Tween 20 and gentle rocking. The tissue was then transferred to 100% methanol and stored at 4°C prior to imaging. Just prior to imaging, gubernacula were cleared by incubation in benzyl alcohol:benzyl benzoate (1:2), transferred to a concavity slide, and cover slipped for viewing. Samples were imaged using an Olympus BX60 digital photomicroscope equipped with ImagePro v6.3 software (Media Cybernetics). Z stacks at 2 μm step sizes were acquired through the entire gubernaculum using a 10X/0.4NA lens. AutoQuant X3 (Media Cybernetics) software was used to generate three-dimensional deconvolution images.

RESULTS

Early Postnatal Migration of the orl Gubernaculum

In previous studies, we observed delayed perinatal inversion of the orl gubernaculum to form the cremaster sac. We defined the extent of cremaster development in dissections of newborn wt and orl males with the aid of intraperitoneal dye to mark its depth and migration. Inverted sacs extending well into the perineum near the site of the future scrotum were visible and contained testes in wt males by 3 days of age (Fig. 1), while aberrant lateral migration of the developing but empty sac was already apparent in orl males by P2–P3. In older orl males, testes are localized within cremaster sacs positioned in the superficial inguinal pouch. Visualization of this abnormal phenotype in the early postnatal period suggests that anatomical distortion of the fetal gubernaculum [10] does not prevent inversion but contributes directly to lateral deviation after birth.

Hormone Receptor mRNA Levels in the Perinatal Gubernaculum

We compared expression of the androgen (Ar) and INSL3 (Rxfp2) receptor mRNA in orl and wt gubernacula isolated at E17, the same gestational age used for hormonal stimulation experiments [8, 9] and at intervals extending up to early puberty (Fig. 2). These data showed that Ar and Rxfp2 levels are highest at E17 and that Rxfp2 expression decreases rapidly as the gubernacular swelling reaction continues; however, Ar expression does not change significantly during this period. Although we found no major differences in Ar expression
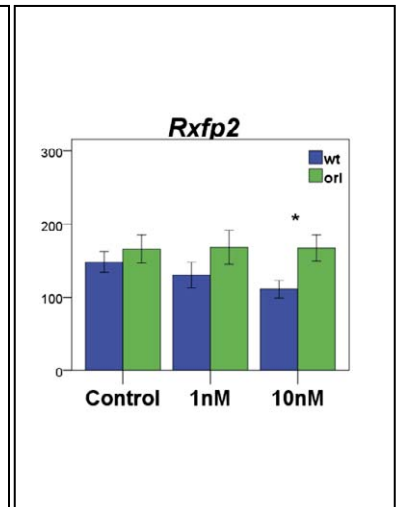
A. Baseline
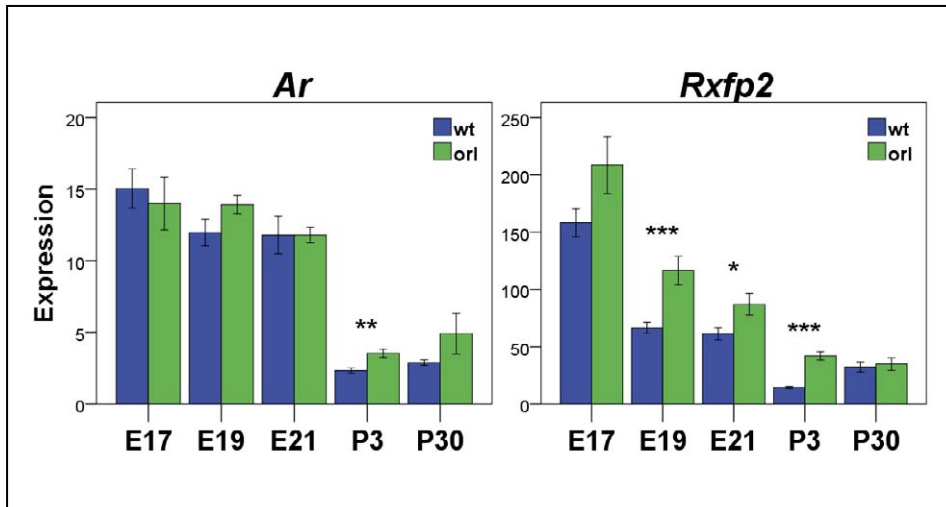
B. Response to INSL3

FIG. 2. Analysis of hormone receptor mRNA levels in fetal wt and orl gubernaculum by qRT-PCR. Data are mean ± SEM, normalized to *Gapdh* expression and quantified relative to rat embryonic total RNA. **A**) *Ar* and *Rxfp2* levels are highest in both strains at E17 and decrease markedly postnatally. Prenatally, *Rxfp2* expression declines significantly ($P < 0.001$ for age and strain effects; $P = 0.3$ for strain-age interaction by UNIANOVA), but no temporal or strain-specific difference in *Ar* expression was observed. Relative to wt, *Rxfp2* expression is increased in orl males at all perinatal time points with significant differences noted between E19 and P3 (*$P < 0.05$; **$P < 0.01$; ***$P < 0.001$ by *t*-test at each time point). **B**) *Rxfp2* levels in E17 wt and orl gubernacular explants cultured with 0–1 and 10 nM INSL3 ($P = 0.01$ and $P = 0.4$ for strain and treatment effect, respectively, by UNIANOVA; $P = 0.015$ for strain comparison by *t*-test at 10 nM exposure).

between wt and orl, *Rxfp2* expression is increased in orl males at all perinatal time points with significant differences first observed at E19 (Fig. 2A). We also observed lower *Rxfp2* expression in wt as compared to orl gubernacular explants following exposure to 10 nM INSL3 with wt and orl exhibiting a differential response to increasing concentrations of hormone (Fig. 2B; $P = 0.01$ for strain and $P = 0.4$ for treatment effects, respectively, by UNIANOVA). The trend of diminishing *Rxfp2* expression in wt gubernaculum explants in response to increasing concentrations of INSL3 was not observed in orl samples. This trend is reminiscent of the significant reduction in gubernacular *Ar* expression after in vitro DHT exposure reported previously [8].

Fetal Testosterone and INSL3 Levels

Testicular testosterone was easily measurable in wt fetuses at E17 (0.29 ± 0.13 ng/testis), peaked at E19 (0.47 ± 0.2 ng/testis), and subsequently declined by E21 (Fig. 3A). In orl fetuses, testosterone levels were reduced significantly to approximately 60% of wt levels at both E17 (0.17 ± 0.05 ng/testis) and E19 (0.30 ± 0.07 ng/testis) but were equivalent to wt by E21. In contrast, mean INSL3 measured in pooled male sera peaked at E17 in wt fetuses (6.0 ± 2.6 ng/ml) but also declined to less than half of peak levels (2.2 ± 0.7 ng/ml) by E21, just prior to inversion of the gubernaculum (Fig. 3B). A secondary rise in serum INSL3 was measured in pubertal wt males at P35. In contrast, mean serum INSL3 also peaked at E17 but remained elevated in orl (5.8 ± 3.8 ng/ml) as compared to wt (3.8 ± 2.0 ng/ml) fetuses at E19, was significantly higher in orl fetuses at E21 (4.0 ± 1.4 ng/ml), and at P35 rose to 8.3 ± 3.1 ng/ml, approximately 2.5 times higher than wt levels (3.2 ± 1.3 ng/ml). The range of INSL3 levels in orl males at P35 (5.2–14.5 ng/ml) was essentially nonoverlapping with levels in wt males at this age (3.2–5.3 ng/ml). Surprisingly, we also observed a peak in serum INSL3 in female fetuses at E17 for both strains, although measurements were highly variable (Fig. 3C). Nevertheless, temporal

variation in INSL3 levels between E16 and E21 was significant for wt females ($P < 0.001$). The source of measurable levels of serum INSL3 in female fetuses exhibiting an expression pattern similar to that seen in males is unknown. While the present studies did not allow us to determine whether a relationship exists between serum INSL3 and *Rxfp2* mRNA expression in vivo, it is noteworthy that both serum INSL3 and *Rxfp2* transcript expression levels fail to decline as precipitously in orl relative to wt rats during the perinatal period.

Sequencing and Expression of Insl3

We identified a susceptibility locus characterized by a wide genomic peak on chromosome 16 telomeric to *Insl3* in a linkage study of orl cryptorchidism (Barthold et al., unpublished results). Because *Insl3* is clearly a strong candidate for cryptorchidism susceptibility, and with the apparent dysregulation of *Rxfp2* and serum INSL3 expression in orl fetuses, we sequenced the exons, intron-exon junctions, and the promoter region of *Insl3* in wt and orl rats. Although we failed to identify any potentially functional variants in the orl genome, we detected a nonconserved C > T polymorphism in the *Insl3* 3′UTR (chr16:18891403 in RGSC 3.4 assembly) that is homozygous in orl and heterozygous in SD rats. Sequences deposited in the Rat Genome Database Variant Visualizer (http://rgd.mcw.edu/rgdweb/front/select.html) [13] indicate that this variant is present in about 20% of genotyped rat strains. We measured *Insl3* mRNA levels in hybrid SD × LE wt fetuses selectively bred for the T/T *Insl3* genotype and found no correlation between carriage of the T/T genotype and *Insl3* mRNA levels in orl and SD × LE males (Fig. 4), suggesting that this variant is not directly associated with variation in *Insl3* levels in the fetal testis. Although the reason for increased expression of INSL3 and *Rxfp2* in orl fetuses remains unknown, these data do not show a consistent association between the *Insl3* polymorphism and *Insl3* mRNA levels nor do they support our hypothesis that *Insl3* represents the
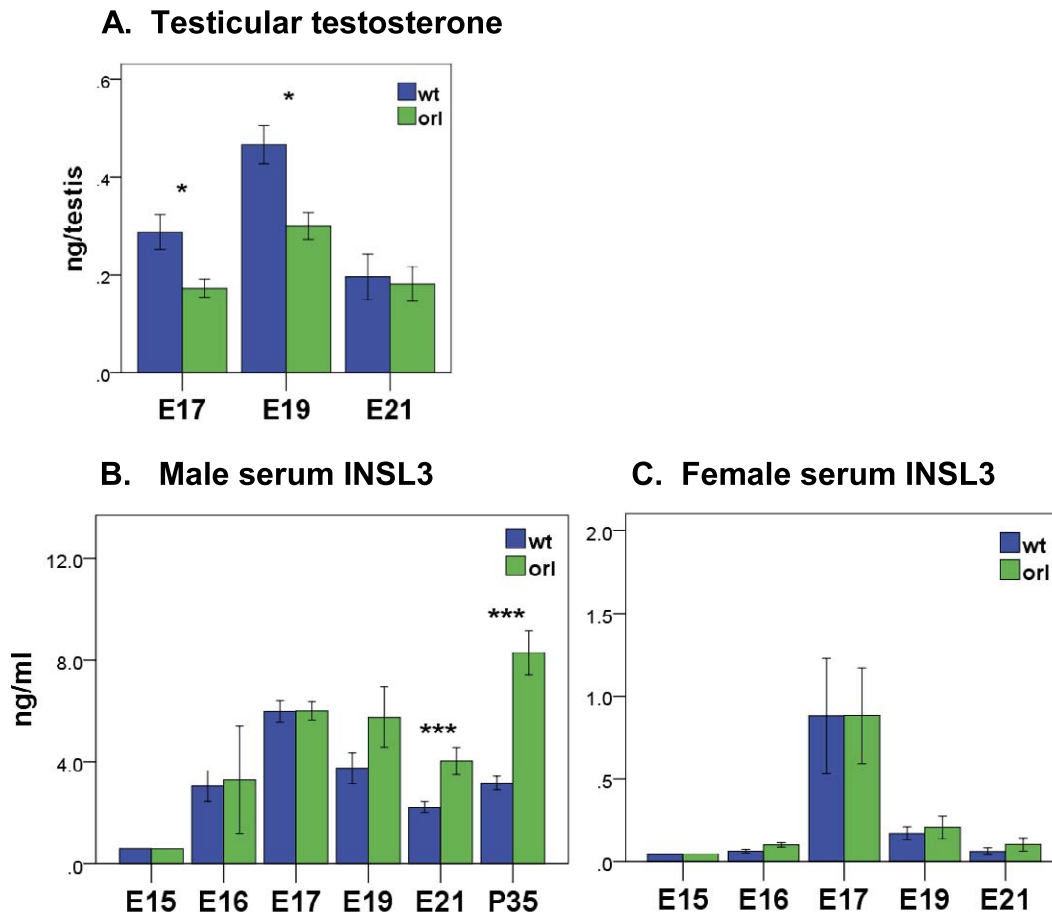
Article 41

A. Testicular testosterone

B. Male serum INSL3

C. Female serum INSL3

FIG. 3. Hormone levels in fetal and postnatal wt and orl rats. **A**) Testicular testosterone (mean ng/testis ± SEM) peaks at E19 ($P < 0.001$ and $P = 0.03$ for age and strain effects, respectively, and $P = 0.8$ for strain-age interaction by UNIANOVA) and is higher in wt than orl males at E17 and E19 (*$P < 0.05$ by *t*-test at each time point). **B**) INSL3 levels peak in males at E17 ($P < 0.001$ and $P = 0.03$ for age and strain effects, respectively, and $P < 0.001$ for strain-age interaction by UNIANOVA) and are significantly different between strains at E21 and P35 (***$P < 0.001$ by *t*-test at each time point). **C**) In females, serum INSL3 shows significant variation with a peak at E17 but no difference between strains ($P < 0.001$ for age and $P = 0.5$ for strain effects by UNIANOVA).

chromosome 16 locus that is linked to increased risk of cryptorchidism in the orl strain.

Characterization of the E17–E19 Gubernacular Transcriptome

To define temporal changes in the gene expression profile of the fetal gubernaculum at the developmental stage used for our previous in vitro hormone stimulation studies, we analyzed pooled gubernacula from wt and orl litters at E17 and E19. We initially identified only 107 probe sets with significant expression changes between wt and orl males at E19 as compared to 4089 differentially expressed E17 probe sets. Hierarchical clustering of the 107 E19 probe sets revealed that two samples (one for each strain) clustered with all the samples in the opposite group and were therefore excluded. Final analyses included five to seven samples from ≥2 litters per group.

We identified 2551 probe sets with significant expression changes between E17 and E19 in wt males. Of these, expression increased at E19 in 1391 and decreased in 1160. Analysis of 1956 identifiers mapped to these probe sets (Supplemental Table S1; Supplemental Data are available online at www.biolreprod.org) using IPA with multiple testing correction yielded functional annotations related almost exclusively to muscle development and function (selected functional categories are listed in Table 1; complete IPA results

are shown in Supplemental Table S2). We identified oxidative phosphorylation, mitochondrial dysfunction, and calcium signaling as significantly overrepresented canonical pathways for the mapped genes differentially expressed between E17 and E19 in the wt gubernaculum (Table 1).

In cross-strain comparisons at both time points, 5833 probe sets (4559 mapped by IPA) were differentially expressed (Supplemental Table S1). Of these, orl transcript expression at E17 and/or E19 was increased for 3193 probe sets (2406 mapped) and decreased for 2237 probe sets (1835 mapped), and strain differences were inconsistent at the two time points for 403 probe sets (318 mapped). We identified many overrepresented functions and canonical pathways in the list of downregulated orl genes that overlap those showing significant changes in expression between E17 and E19 in wt males (Table 1) but no overrepresented functional annotations and only one pathway (assembly of RNA polymerase II complex, $P = 0.02$) in the analysis of upregulated orl genes. Many of the same muscle-related annotations are also overrepresented in the list of probe sets with ≥1.5- and/or 2-fold differential expression between strains (orl-wt 1.5-fold and orl-wt 2-fold, Table 1). We also identified organization of ECM as a potentially relevant overrepresented functional category in the analysis of transcripts with at least 1.5-fold differential expression between strains. This category is also enriched in a list of transcripts that are responsive to both 10 and 30 nM DHT exposure in vitro [8].
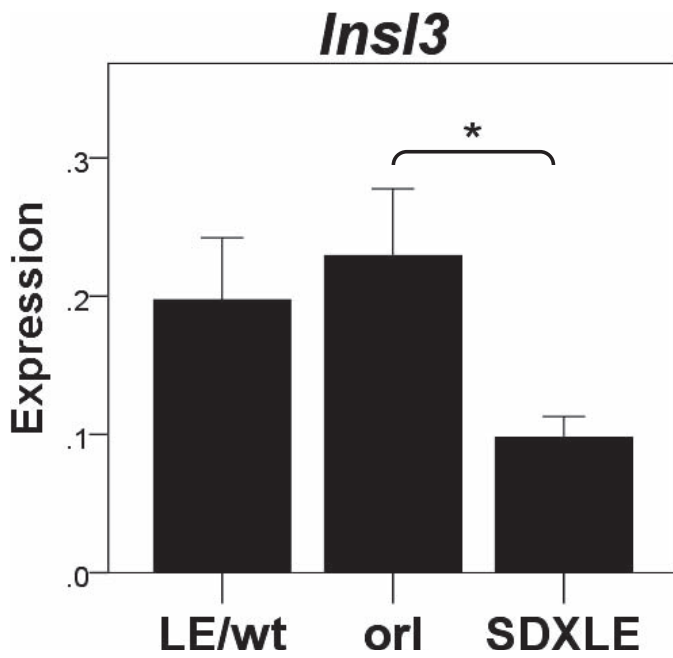
Insl3

FIG. 4. Genotype-specific *Insl3* mRNA levels (mean ± SEM) in E19 testis by qRT-PCR. Data are mean ± SEM, normalized to *Gapdh* expression and quantified relative to rat embryonic total RNA. Expression of testicular *Insl3* mRNA is not significantly different between wt LE (Long Evans) males that are homozygous for the consensus (C/C) *Insl3* 3′UTR allele (chr16:18891403, RGSC 3.4 assembly) and orl males homozygous for the alternative allele (T/T), but testicular *Insl3* expression is significantly reduced compared to orl (*$P < 0.05$) in homozygous T/T male pups generated by a SD (Sprague-Dawley) × LE intercross.

Supplemental Table S3 includes all mapped genes in the muscle-specific categories that are included in both the wt E17–E19 and orl-wt 1.5-fold lists. Most (64%) of the transcripts that are more highly expressed at E17 participate in muscle development/myogenesis or muscle organization, while the majority (84%) of those more highly expressed at E19 are involved in muscle contraction and/or function. Many orl transcripts are expressed at lower levels at E17 and/or fail to achieve wt developmental expression levels by E19. The majority of muscle-related transcripts did not show significant

expression changes in response to DHT or INSL3 exposure at E17 [8, 9] (last two columns of Supplemental Table S3), suggesting that altered muscle-specific gene expression at this developmental stage is not directly regulated by hormones. Supplemental Table S4 shows the expression levels of genes annotated to organization of ECM by IPA analysis (Table 1) and those on the microarray chip that encode ECM components. Interestingly, orl expression at E17 is reduced for the majority of ECM transcripts but reaches or exceeds normal levels by E19.

We used IPA to map and compare differentially expressed probe sets from the present and prior developmental studies of the fetal gubernacular transcriptome [11]. Although the chips we used in the previous study interrogated only a subset of the transcripts that were analyzed in the present experiments and the prior samples were harvested at different time points and were not pooled, a total of 1390 IPA-mapped genes (of 4066 and 2840 unique, differentially expressed genes in the present and prior experiments, respectively) were identified in both studies. Strain-specific expression differences were completely concordant for 677 of 1390 genes; of these, expression was increased in the orl gubernaculum in 323 and decreased in 354. When we analyzed these core lists representing strain differences consistent between experiments, the most prominent overrepresented functions and pathways include those related to cytoskeleton-dependent processes (e.g. cell motility and survival) and muscle for over- and underexpressed transcripts, respectively (Table 2 and Supplemental Table S2), supporting our previous observations [11]. They also show altered expression of transcripts involved in Wnt signaling, an apparent downstream target of both androgen and INSL3 [7, 8], in the orl gubernaculum.

Overlap of the Unexposed and Hormone-Exposed Fetal Gubernaculum Transcriptome

Because muscle development is hormonally regulated in the gubernaculum [6, 7] and our data suggest altered expression of hormone receptor and muscle-specific transcripts in the orl fetus, we searched for overlap between hormone-responsive and differentially expressed orl probe sets. We compared IPA-mapped genes uniquely responsive to DHT or INSL3 [8, 9] with IPA-mapped genes from the present experiments that are

TABLE 1. Selected functional and pathway annotations for differentially expressed transcripts in wt and orl fetal gubernaculum.[a]

Parameter	wt E17–E19[b]	orl < wt[c]	orl-wt 1.5-fold[d]	orl-wt 2-fold[e]
Diseases or functions				
Muscle contraction	2.3E−12	5.9E−04	1.5E−06	6.1E−03
Development of muscle	9.8E−09	2.7E−03	2.6E−04	8.6E−05
Function of muscle	8.9E−06	8.8E−03	3.0E−02	
Dystrophy of muscle	4.9E−04	5.3E−03		
Congenital myopathy	1.5E−03	2.6E−06		1.4E−02
Organization of muscle	2.8E−02		1.3E−02	8.6E−05
Formation of myofibrils	5.0E−02			5.1E−03
Organization of extracellular matrix			1.2E−02	
Pathways				
Oxidative phosphorylation	5.9E−06	1.6E−02		
Mitochondrial dysfunction	1.7E−04	1.6E−02		
Calcium signaling	5.7E−03			
Superpathway of cholesterol biosynthesis		1.6E−02		
Regulation of cellular mechanics by calpain protease		1.6E−02		

[a] Values represent Benjamini-Hochberg corrected *P* values for selected diseases or functions and for all pathways identified using IPA analysis.
[b] List of probe sets differentially expressed between E17 and E19 in wt gubernaculum.
[c] List of differentially expressed probe sets with lower expression in orl versus wt at E17 and/or E19.
[d] List of differentially expressed probe sets with 1.5-fold difference in expression between orl and wt at E17 and/or E19.
[e] List of differentially expressed probe sets with 2-fold difference in expression between orl and wt at E17 and/or E19.

TABLE 2. Functional analysis of gubernacular transcripts showing consistent strain-specific expression patterns.[a]

Parameter	orl > wt	orl < wt
Diseases or functions*		
Migration of cells	1.5E−06	
Proliferation of cells	1.5E−06	
Cell viability	2.9E−04	
Formation of cellular protrusions	1.3E−03	
Microtubule dynamics	1.5E−03	
Muscle contraction		1.1E−09
Development of muscle		2.6E−04
Function of muscle		7.6E−04
Dystrophy of muscle		1.9E−03
Myopathy		8.7E−06
Pathways**		
Role of osteoblasts, osteoclasts, and chondrocytes in rheumatoid arthritis	1.9E−03	
Role of macrophages, fibroblasts, and endothelial cells in rheumatoid arthritis	2.5E−03	
Wnt/β-catenin signaling	5.8E−03	
Glucocorticoid receptor signaling	3.7E−02	
Colorectal cancer metastasis signaling	4.2E−02	
Oxidative phosphorylation		2.5E−13
Mitochondrial dysfunction		6.3E−12

[a] IPA analysis of mapped genes showing consistent patterns of differential expression between wt and orl fetal gubernaculum in prior [11] and present microarray experiments; *selected, **all pathways represented by ≥ 10 molecules in the list of differentially expressed transcripts.

differentially expressed in orl relative to wt gubernaculum at E17 and/or E19. Overall, 42% of DHT-responsive and 41% of INSL3-responsive genes mapped by IPA from our existing lists of hormone-responsive probe sets are also differentially expressed in the orl gubernaculum at E17 and/or E19. However, orl expression levels correlate negatively with hormonal response for significantly more DHT-regulated (247 of 884, 28%) than INSL3-regulated (225 of 1443, 16%) genes ($P < 0.0001$). This relationship is illustrated using heat maps (Fig. 5) showing only the overlapping transcripts with at least a 2-fold response to INSL3 and/or DHT. The majority of these most highly DHT-responsive transcripts are differentially expressed in the orl gubernaculum in a pattern suggesting either a reduced androgen response or reduced exposure to androgen. These data are consistent with our previous gene expression profiling that identified enrichment of genes related to androgen signaling in the orl gubernaculum [11]. In contrast, orl expression levels are congruent with hormonal response for significantly more INSL3-regulated (338 of 1443, 23%) than DHT-regulated (11 of 884, 12%) genes ($P < 0.0001$), particularly those that are upregulated at E19 (Fig. 5) suggesting an increased INSL3-specific transcriptional response in orl fetuses. These gene expression data are also consistent with our observations that testicular testosterone is reduced, implying decreased exposure to androgen in vivo, and serum INSL3 and *Rxfp2* mRNA expression are increased in the orl fetus.

Hormonal Response of the orl Gubernaculum in Organ Culture

We used existing knowledge of mRNAs that are responsive to DHT and/or INSL3 to search for potential differences in the hormonal responsiveness of the orl gubernaculum. Using the same methodology as previously reported [8, 9], we analyzed transcript levels following exposure of E17 gubernaculum pairs to varying concentrations of hormone for 24 h following a 24-h

washout period. We noted an orl response that is similar to wt following exposure to 10 or 30 nM DHT for most genes, although the response appears to be less pronounced for *Chrdl2* and *Wnt4* at the more physiologic concentration of 10 nM [8] (Fig. 6). Unlike the wt response, we did not observe a significant decrease in *Myh7* or increase in *Slit3* expression, but did observe a significant reduction in *Sfrp2* expression in orl gubernaculum in response to DHT. *Slit3* is located in one of several linkage peaks identified in our genomic studies (Barthold et al., unpublished results) and is therefore a candidate risk allele for orl cryptorchidism susceptibility. These data suggest a generally intact transcriptional response of the orl gubernaculum to exogenous androgen, consistent with normal prenatal levels of *Ar* mRNA expression (Fig. 2).

In contrast, we observed increased sensitivity of the orl gubernaculum to INSL3 (Fig. 7). For all the genes, the threshold INSL3 concentration yielding a significant response was 10-fold lower (at 0.1 or 1 nM) in orl as compared to wt (1 or 10 nM) and reminiscent of the enhanced response that we observed for the INSL3-responsive transcripts *Wnt4*, *Bmp3*, and *Chrdl2* in E17 female gubernacula [9]. Additionally, for *Nptx2*, *Crlf1* ($P = 0.06$), and *Bmp3*, we observed a paradoxical decrease in expression following exposure to 0.1 nM INSL3. These data provide additional support for the existence of enhanced INSL3/RXFP2 signaling activity in the orl gubernaculum.

Strain-Specific Expression of Hormone-Responsive Transcripts in Fetal Gubernaculum

We used qRT-PCR to analyze developmental gene expression in freshly isolated fetal gubernacula, focusing primarily on transcripts that we validated as hormonally responsive in wt and/or orl experiments. These include *Pnoc*, *Nptx2*, *Bmp3*, and *Wnt5a* (upregulated by INSL3 in wt); *Has2* (upregulated by DHT); *Slit3* (upregulated by DHT in wt only); *Adh1*, *Crlf1*, and *Chrdl2* (upregulated by INSL3 and DHT); *Bmp4*, *Tgfb2*, and *Cxcl12* (downregulated by DHT); and *Wnt4* (upregulated by INSL3 and downregulated by DHT). Upregulated *Adh1* response for both hormones is significant based on the array data but was validated by qRT-PCR for DHT only [8]. These data (Fig. 8) indicate that developmental expression of hormone-responsive genes is dysregulated in the orl fetal gubernaculum. All of the transcripts that we studied by qRT-PCR except *Has2* (data not shown) showed altered expression levels in orl at E17 and/or E19. The qRT-PCR results also confirm the microarray data by validating significant differences or at least concordant trends in expression between strains for all the targets except *Slit3*, a transcript that is significantly upregulated following DHT exposure in wt but not in orl gubernaculum. For *Slit3*, the microarray and qRT-PCR results are inconsistent, suggesting decreased (Supplemental Table S3) and increased (Fig. 7) mRNA expression, respectively, in orl gubernaculum.

As noted above, the developmental expression of many transcripts suggests a reduced androgenic response and/or increased INSL3 response in orl samples. Specifically, transcripts downregulated by DHT, including *Bmp4*, *Sfrp2*, *Tgfb2*, and *Cxcl12*, are increased in the E17 and/or E19 orl gubernaculum, and expression of the DHT-upregulated gene *Adh1* was decreased at E17. In contrast, expression of all INSL3-upregulated transcripts except for *Nptx2* is increased in E19 orl gubernaculum. In summary, the data suggest that the orl gubernaculum responds normally to androgen stimulation in vitro but that transcript expression in the intact orl fetus suggests reduced androgen response, which may in part be due
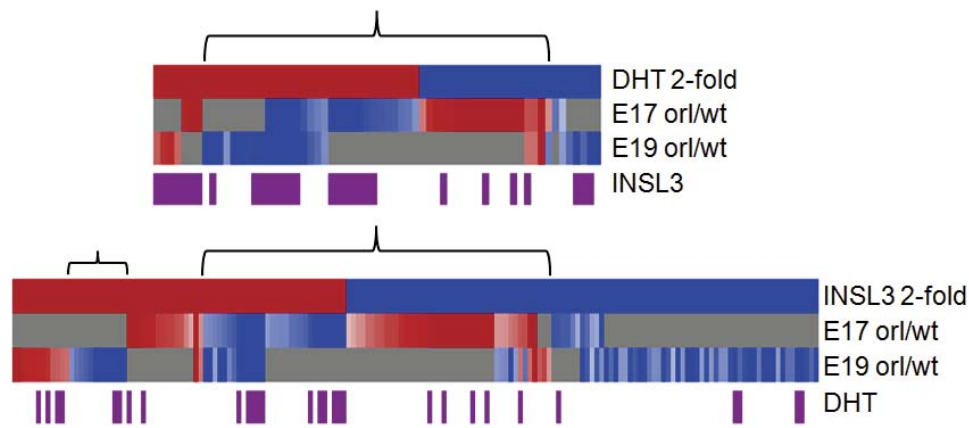
FIG. 5. We performed hierarchical clustering of differentially expressed probe sets with at least a 2-fold expression change following exposure of wt E17 gubernacular explants to INSL3 (top) or DHT (bottom). The top row of each cluster shows probe sets that were upregulated (red) and downregulated (blue) following exposure to each hormone. The bottom two rows show matched probe sets that are upregulated (red), downregulated (blue), or not differentially expressed (gray) in orl gubernacula at E17 and E19. Bottom panels (purple) identify probe sets also responsive to the alternative hormone (DHT or INSL3). Brackets indicate probe sets that are upregulated or downregulated in response to each hormone but show lower or higher expression, respectively, in orl at E17 and/or E19.

to reduced androgen production at E17–E19. In contrast, the increased sensitivity of the orl gubernaculum to INSL3 in vitro correlates with increased expression of INSL3-responsive transcripts in untreated orl gubernacula.

Three-Dimensional Imaging of the wt and orl Fetal Gubernaculum

Myosin heavy chain immunostaining of microdissected gubernacula at E21 confirms an orthogonal pattern of peripheral muscle fibers with a distal opening at the insertion of the gubernacular cord as noted previously [18]. With optical tissue clearing, we were able to observe a more complex pattern than has been previously appreciated, including a longitudinal gap in the muscle (Fig. 9) adjacent to a medial peritoneal fold that connects to the Wolffian duct system. The wt E21 gubernacula show a regularly spaced orthogonal muscle fiber distribution, a well-demarcated medial longitudinal muscle gap, and a symmetric ovoid shape. In contrast, although some orl gubernacula appear normal, we observed a range of phenotypes that include varying degrees of obliquity, muscle pattern asymmetry, thinning, an aberrant horizontal muscle gap, and focal absence of muscle (Fig. 9). These phenotypes may reflect abnormal cellular migration, cellular hypoplasia, defects in signaling pathways that regulate muscle patterning, and/or inadequate or aberrant ECM deposition and swelling. Defective muscle pattern formation may contribute to mechanical weakness and dysmotility during inversion of the gubernaculum.

DISCUSSION

Cryptorchidism is a common developmental anomaly of unknown but presumed multifactorial etiology. The orl rat is a unique tool to facilitate understanding of the genetic basis of this complex disease. As in most clinical cases, the orl phenotype appears to be relatively mild, nonsyndromic, and unrelated to mutations in *Insl3* or *Rxfp2* or to major testicular hormone deficiency or dysgenesis [19]. Therefore, this model may provide insight into pathways downstream of hormonal signaling that lead to developmental disruption of the gubernaculum and consequent cryptorchidism. To define the etiology of orl cryptorchidism, our laboratory has performed complementary studies of gubernacular development that include phenotyping, developmental gene and hormone expression profiling, analysis of hormone-responsive transcript expression, and linkage analysis coupled with whole genome sequencing to identify causative variants at genomic loci.

The mild anatomical defects that we observed previously in microdissections of the prenatal orl gubernaculum, including elongation and narrowing followed by delayed inversion [10], progress to aberrant lateral migration that is easily visible by Day 3 of life. We observe focal defects in muscle patterning within the fetal orl gubernaculum that do not prevent inversion but likely predispose to mislocalization of the cremaster sac. The testis ultimately migrates into the aberrantly located sac and both continue to grow into adulthood. These observations suggest that crucial events required for completion of testicular descent occur around the time of birth in rats, as in humans. Moreover, the orl model is likely relevant to human cryptorchidism because ectopic location of testes in the superficial inguinal pouch is a common phenotype in boys. Postnatal cremaster muscle growth in rats has been compared to limb bud development [18] but occurs after the orl phenotype is established, is not inhibited by antiandrogens, and is at least partially dependent on testicular growth [20].

The role of the human cremaster in facilitating testicular descent is not well understood, but a detailed histological analysis suggests that striated muscle fibers within and around the migrating gubernaculum have several planes of orientation [4]. The present observations confirm that the normal rat cremaster is open at the gubernacular tip, contains oblique and orthogonal muscle layers, and has a longitudinal muscle gap (as in humans), suggesting the possibility that peristaltic activity may contribute to gubernacular inversion. In implicating developmental muscle patterning as a key element in normal cremaster development and function, the present data are consistent with clinical data showing association of cryptorchidism with neuromuscular disorders and anomalies of the muscular abdominal wall and diaphragm [21–25]. Interestingly, transgenic inactivation of *Dlg1* (discs large homolog 1), encoding a protein that functions in cellular polarity, adhesion, and proliferation, is associated with both incomplete fetal testicular descent [26] and disorganization of ureteral muscle with impaired peristalsis [27]; gubernacular
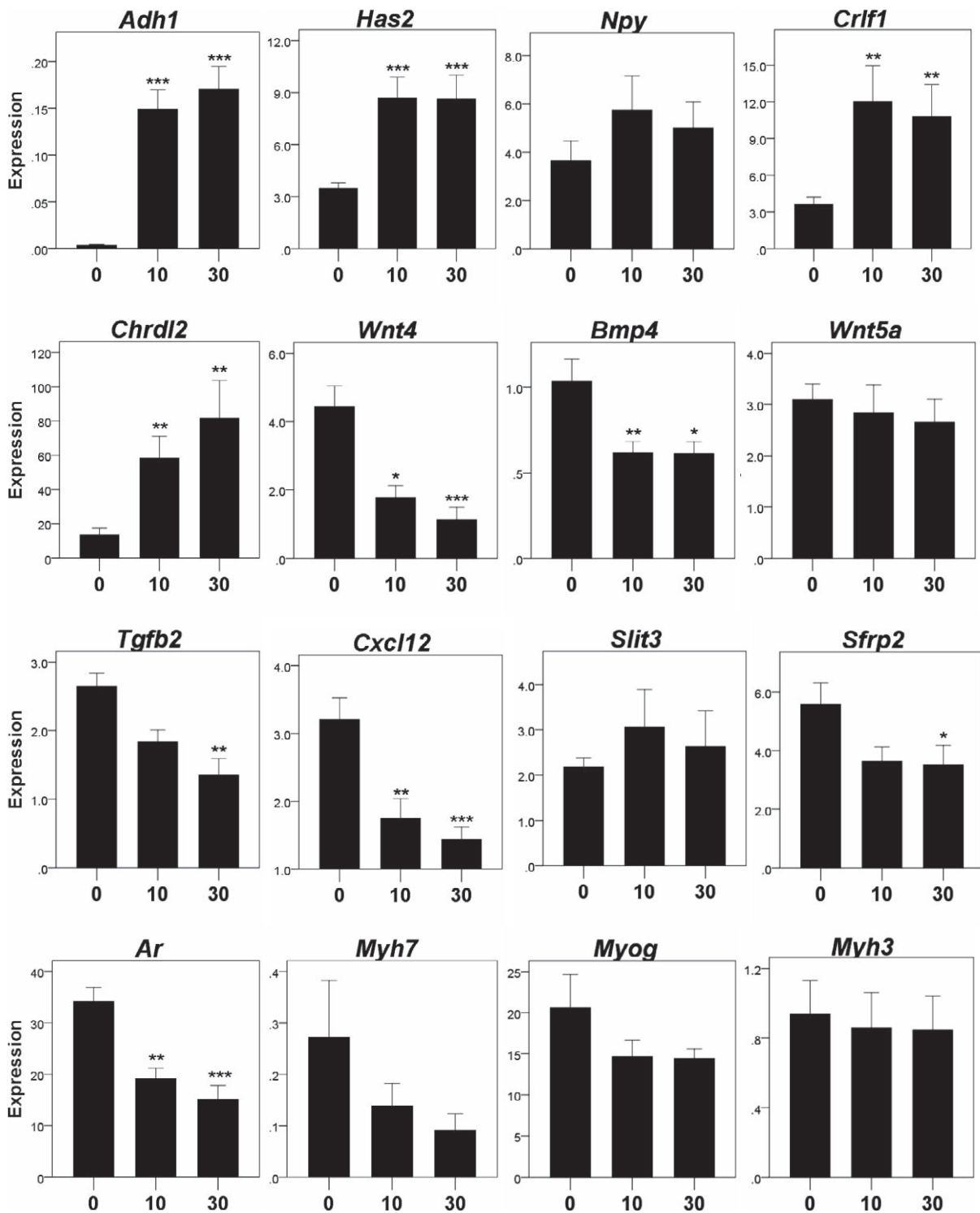
FIG. 6. Response of the orl fetal gubernaculum to dihydrotestosterone (DHT). E17 orl gubernacular explants were exposed to DHT (0, 10, and 30 nM) in culture for 24 h following a 24-h washout period. Data show expression of target genes (mean ± SEM), normalized to *Gapdh* expression and quantified relative to rat embryonic total RNA. Results are organized to mirror previous data using wt gubernacula [8]. *Adh1*, alcohol dehydrogenase 1; *Has2*, hyaluronan synthase; *Npy*, neuropeptide Y; *Crlf1*, cytokine receptor-like factor 1; *Chrdl2*, chordin-like 2; *Wnt4*, wingless-related MMTV integration site 4; *Bmp4*, bone morphogenetic protein 4; *Wnt5a*, wingless-related MMTV integration site 5a; *Tgfb2*, transforming growth factor beta 2; *Cxcl12*, chemokine (C-X-C motif) ligand 12; *Slit3*, slit homolog 3; *Sfrp2*, secreted frizzled-related protein 2; *Ar*, androgen receptor; *Myh7*, myosin, heavy chain 7, cardiac muscle, beta; *Myog*, myogenin; and *Myh3*, myosin, heavy chain 3, skeletal muscle, embryonic. $*P < 0.05$, $**P < 0.01$, and $***P < 0.001$ relative to 0 nM.

development, however, was not studied. Similarly, reduction or failure of muscle development within the gubernaculum is a prominent feature in transgenic mice with inactivation of embryonic patterning genes, such as *Ctnnb1*, *Notch*, *Wnt5a*, and *Hoxa11* [7, 28–30]. The more subtle pathology of the orl cremaster that becomes apparent with three-dimensional imaging provides us with the opportunity to better define the functional properties of this surprisingly complex structure.
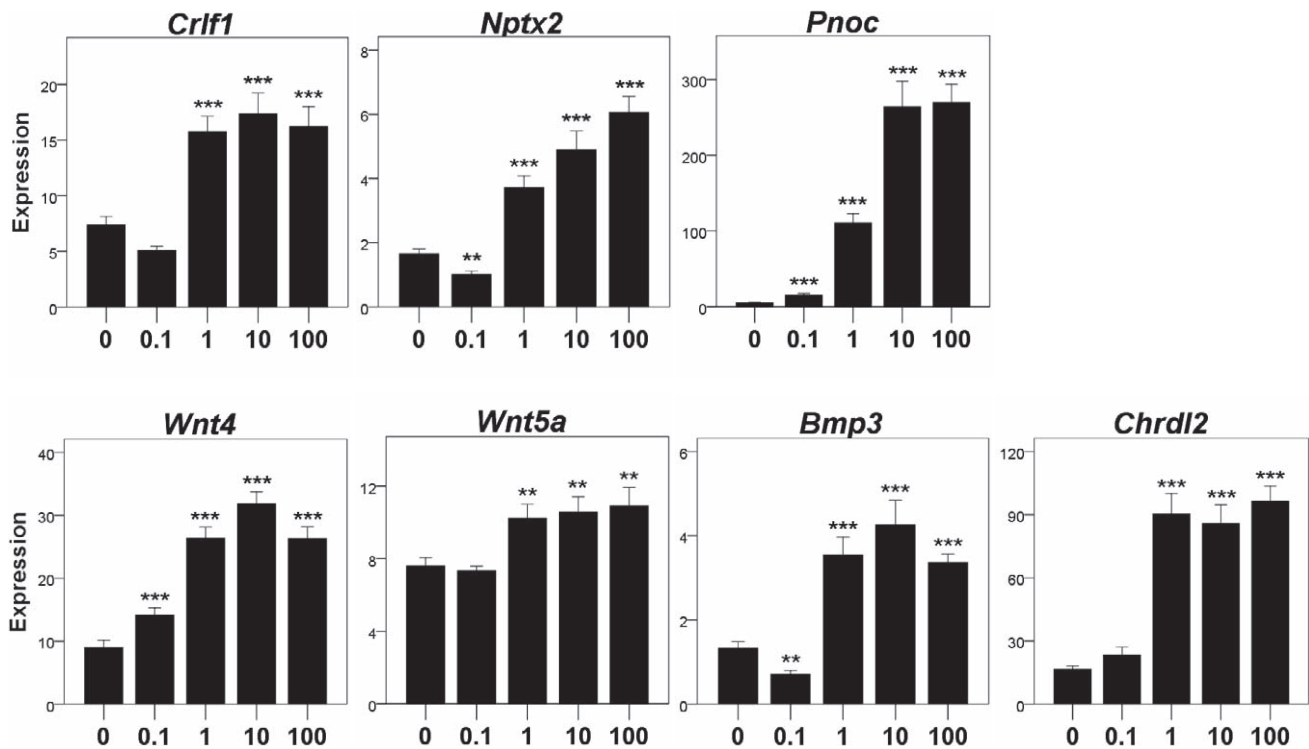
FIG. 7.   Response of the orl fetal gubernaculum to insulin-like 3 (INSL3). E17 orl gubernacular explants were exposed to INSL3 (0, 0.1, 1, 10, and 100 nM) in culture for 24 h following a 24-h washout period. Data show expression of target genes (mean ± SEM), normalized to *Gapdh* expression and quantified relative to rat embryonic total RNA. Results are organized to mirror previous data using wt gubernacula [9]. *Crlf1*, cytokine receptor-like factor 1; *Nptx2*, neuronal pentraxin II; *Pnoc*, prepronociceptin; *Wnt4*, wingless-related MMTV integration site 4; *Wnt5a*, wingless-related MMTV integration site 5a; *Bmp3*, bone morphogenetic protein 3; and *Chrdl2*, chordin-like 2. *$P < 0.05$, **$P < 0.01$, and ***$P < 0.001$ relative to 0 nM.

We hypothesized that anomalous development and altered mechanical properties of the prenatal gubernaculum set the stage for testicular maldescent. However, the developmental mechanisms of atypical muscle development in the orl gubernaculum remain poorly defined. Early studies suggesting that peripheral migration of mesenchymal myoblasts contributes to cremaster muscle formation [31] are supported by data showing desmin-positive myogenic cells in the central core of the gubernaculum that persist in conditional $Rxfp2^{-/-}$ mouse fetuses [7]. In orl E21 fetuses, cremaster patterning may be distorted, focally absent, or asymmetric and the gubernaculum is narrow, suggesting that defects are present in both alignment of muscle and completion of the swelling reaction. Indeed, compared to wt, the gene expression profile of the orl gubernaculum shows increased expression of genes related to cellular migration and reduced expression of ECM- and muscle-related genes. While these data suggest that gubernacular development is delayed and/or deficient in the orl fetus, they do not provide insight into the primary cause of the defect but nonetheless inform the search for causative alleles. Swelling of the mesenchymal core is subtle in rodents but if insufficient, may affect the shape and mechanical properties of the gubernaculum and its capacity for correct inversion. In larger mammals, the PG content of the fetal gubernaculum is measurable and in the pig consists of dermatan sulfate (~50%), hyaluronic acid (~30%), and chondroitin and heparan sulfates (~10% each) at the peak of the swelling reaction [32]. Matrix constituents facilitate swelling due to osmotic pressure but may also play an important role in activation of extracellular signaling pathways that promote cellular proliferation, migration, and muscle patterning such as Slit/Robo, Bmp, and Wnt signaling [33–35]. ECM characteristics are known to correlate with the phenotype of migrating cells and may influence the behavior of cremaster muscle precursors [36].

Gubernacular enlargement and muscle patterning fail to varying degrees in the absence of INSL3 or androgen signaling, suggesting a role for testicular hormones in the swelling reaction of the gubernacular mesenchyme and in cremaster muscle development. While the consequence of loss of INSL3/RXFP2 signaling is more severe, the developmental effects of INSL3 and androgens appear to be synergistic, unique within the developing gubernaculum and not required for development of other muscles. The data of Kaftanovskaya et al. [7] suggest that INSL3/RXFP2 regulates downstream pathways including Wnt and Notch signaling in the fetal gubernaculum and also promotes maintenance of AR$^+$ cells and their migration into the mesenchymal core. These authors also hypothesize that AR$^+$ cells are responsible for changes in ECM production and organization that define the gubernacular swelling reaction [7] and note that ECM-specific gene expression is altered in GU-ARKO males [6]. A notable phenotype in $Rxfp2^{-/-}$ mice is aberrant localization of muscle cells within the gubernacular core, suggesting failure of migration to their proper location peripherally [7]. It is important to note that the role of these hormone pathways in facilitating myogenesis is limited to mesenchymal cells because conditional deletion of Ar or $Rxfp2$ in committed muscle cells has no phenotypic effect [7, 8]. These data strongly support a role for both INSL3 and androgen as master regulators of cellular proliferation, migration, ECM production, and muscle patterning within the fetal gubernaculum.

To investigate whether reduced hormone production and/or response occurs in the orl fetus, we measured levels of testicular and serum hormones and their target hormone receptors during peak development of the gubernaculum.

A. DHT-responsive transcripts
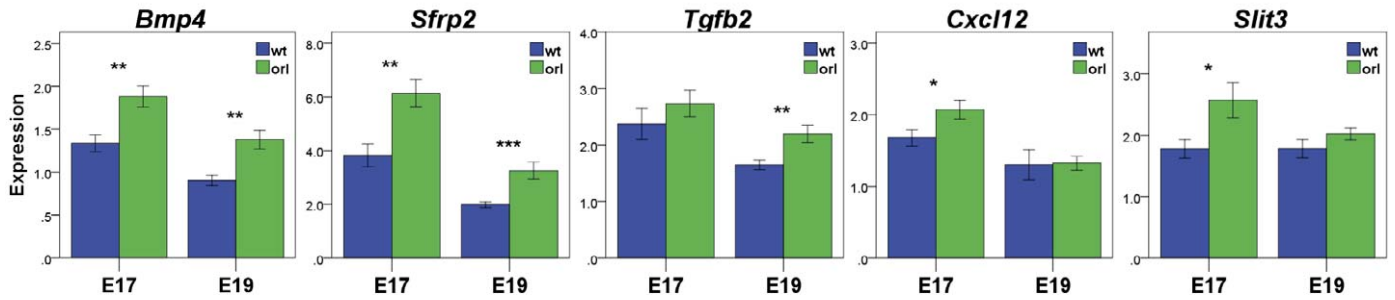
B. INSL3-responsive transcripts
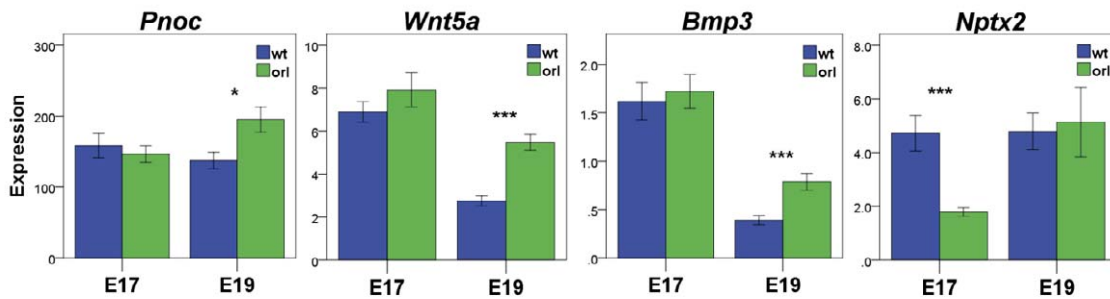
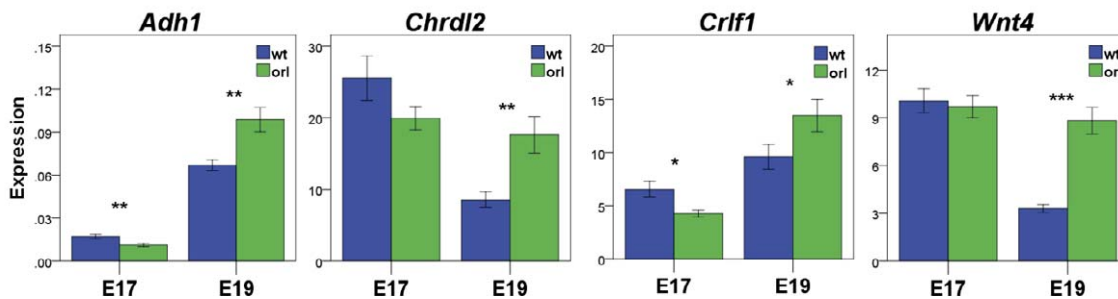## C. DHT- & INSL3-responsive transcripts

FIG. 8. Comparative expression of DHT- and INSL3-responsive transcripts [8, 9] in orl and wt gubernaculum at E17 and E19. Data show expression of target genes (mean ± SEM), normalized to *Gapdh* expression and quantified relative to rat embryonic total RNA. **A**) DHT-responsive transcripts: *Bmp4* (bone morphogenetic protein 4), *Sfrp2* (secreted frizzled-related protein 2), *Tgfb2* (transforming growth factor beta 2), and *Cxcl12* (chemokine [C-X-C motif] ligand 12) are downregulated by DHT in both strains and *Slit3* (slit homolog 3) is upregulated by DHT in wt only. **B**) INSL3-responsive transcripts: *Pnoc* (prepronociceptin), *Wnt5a* (wingless-related MMTV integration site 5a), *Bmp3* (bone morphogenetic protein 3), and *Nptx2* (neuronal pentraxin II) are upregulated by INSL3 in both strains. **C**) DHT- and INSL3-responsive transcripts: *Adh1* (alcohol dehydrogenase 1), *Chrdl2* (chordin-like 2), and *Crlf1* (cytokine receptor-like factor 1) are upregulated by INSL3 and DHT, and *Wnt4* (wingless-related MMTV integration site 4) is upregulated by INSL3 and downregulated by DHT. $*P < 0.05$, $**P < 0.01$, and $***P < 0.001$.

These data suggest that testicular testosterone production is reduced in the orl fetus during the androgen-sensitive period of gubernaculum development, and additional studies (Barthold et al., unpublished results) suggest that allelic variation at a chromosome 6 locus linked to cryptorchidism is a modifier of testicular steroidogenesis. However, the reduction in orl testicular testosterone is relatively modest and, in isolation, may not be biologically significant. Testosterone levels in fetal rats are variable and lower in the LE strain [37] and depend on fetal position within the uterine horn [38]. Moreover, a greater magnitude of suppression than seen in the orl fetus, for example, due to fetal phthalate exposure, does not necessarily induce cryptorchidism in other rat strains [39]. Nevertheless, we observed impaired expression of transcripts that are androgen targets in the orl gubernaculum despite normal *Ar* mRNA levels and in vitro response of the orl gubernaculum to
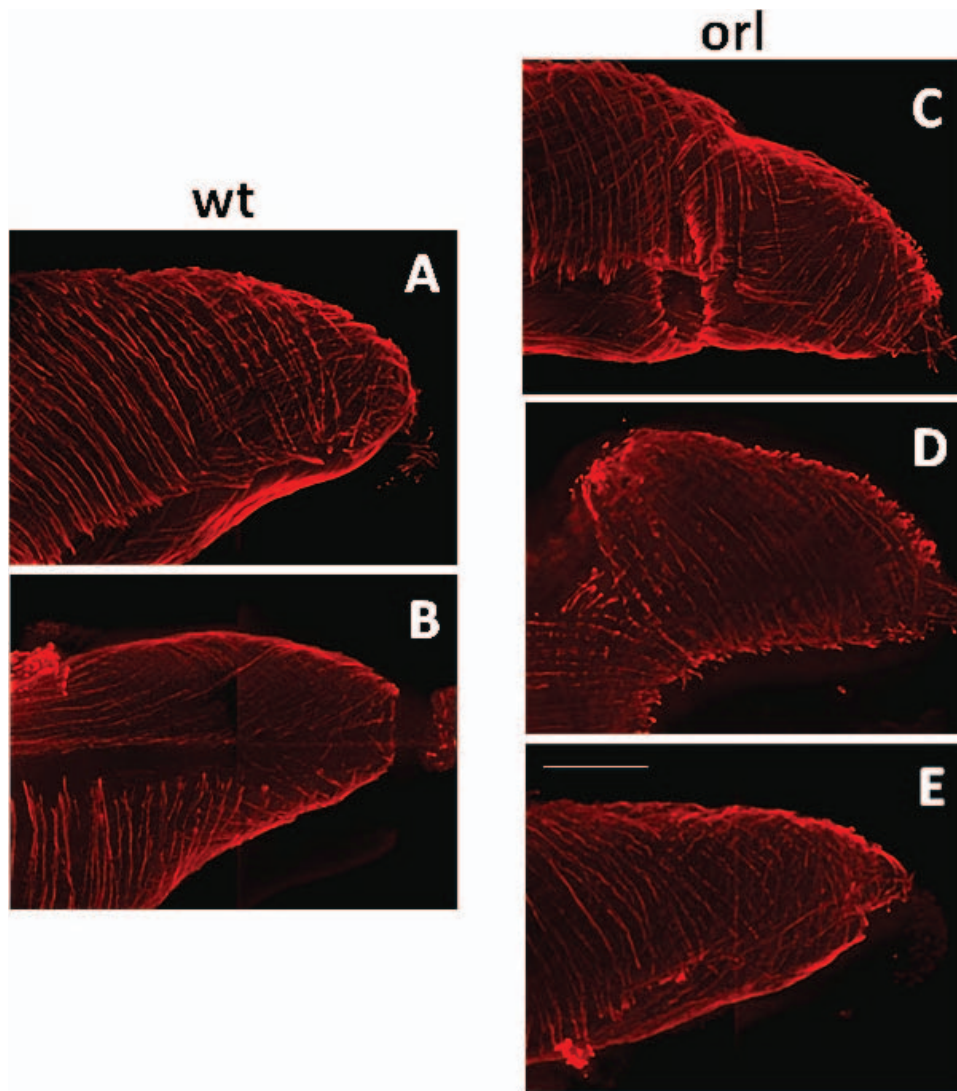
FIG. 9. The three-dimensional muscle pattern of wt and orl gubernacula at E21 (original magnification ×10). Deconvoluted images of fixed whole mount gubernacula were acquired following optical clearing of samples using a benzyl alcohol:benzyl benzoate protocol and immunostaining with labeled A4.1025 myosin heavy chain-specific antibody. Both wt and orl gubernacula show an orthogonal fiber distribution of the two intrinsic muscle layers and a longitudinal gap in the muscle that corresponds to the location of the medial peritoneal fold that connects the gubernaculum to the Wolffian duct system. Wt E21 gubernacula show regularly spaced muscle fibers, a well-demarcated longitudinal muscle gap (visible inferiorly in **A** and en face in **B**) and a symmetric ovoid shape. Selected orl gubernacula (**C**–**E**) show various muscle pattern defects including a transverse muscle gap (**C**), localized absence of muscle and shape asymmetry (**D**), and flattening and focal muscle fiber irregularity (**E**). Bar = 200 μm.

DHT. Some of these targets encode ECM proteins and morphogens, including those in the Wnt pathway. It is possible that further reduction in testosterone levels in a strain with naturally low levels produces a threshold effect or synergizes with risk alleles that target downstream androgen and/or INSL3 signaling to yield a higher cryptorchidism risk in the orl strain.

Slit3 is an androgen-responsive gubernacular gene that may amplify the effects of reduced testosterone production because its transcriptional response to DHT and baseline expression are dysregulated in the orl fetus. SLIT3 is a secreted protein involved in cytoskeletal regulation, cell migration, and muscle patterning that uses heparan and/or chondroitin sulfate-modified PGs as cofactors and, depending on cellular context, can inhibit Wnt and SDF1/*Cxcl12* signaling [35, 40, 41]. Transgenic deletion of *Slit3* and heparan sulfate deficiency both produce congenital diaphragmatic hernia in mice [42, 43], a phenotype associated with cryptorchidism in up to 30% of cases [21]. The existence of variably penetrant renal and ureteral anomalies in *Slit*$^{-/-}$ mice [43] suggests that the intermediate mesoderm is an important SLIT3 developmental target. In addition, *Slit3* interacts with *Frem1* [44], the causative gene for Fraser syndrome, which includes cryptorchidism in 31.5% of males [45]. Drosophila slit acts sequentially as a repellant and an attractant during the process of muscle cell attachment [46]. These data support a potential role for SLIT3 as an extracellular molecule that may direct muscle cell migration and pattern formation in the developing rat gubernaculum.

We showed previously that *Ar* mRNA expression in cultured wt gubernaculum is inversely correlated with androgen exposure [8]. Because we used an embryonic RNA standard as a calibrator for qRT-PCR to allow direct comparison of transcript-specific expression across experiments, the present data provide independent confirmation in the orl strain that *Ar* mRNA levels increase >2-fold with androgen withdrawal and decline to baseline in response to

DHT exposure. In addition, the developmental pattern of *Ar* mRNA expression (Fig. 2) and DHT response (Fig. 5 and reference [8]) is comparable in orl and wt fetuses. Therefore, the moderate reduction in testicular androgen production that we observed does not appear to alter *Ar* mRNA expression or the responsiveness of the orl gubernaculum to exogenous hormone.

Surprisingly, we observed increased levels of both INSL3 in serum and *Rxfp2* mRNA in the gubernaculum beginning at E19, failure of *Rxfp2* downregulation by INSL3, and increased expression of INSL3-responsive transcripts in orl fetuses. We did not assess RXFP2 protein expression in the orl gubernaculum because the available antibodies have not shown consistent results [47]. These differences occur after peak expression and likely maximal developmental INSL3/RXFP2 signaling activity, and therefore are unlikely to contribute to the pathogenesis of cryptorchidism in this strain. Moreover, transgenic overexpression of INSL3 beginning in fetal life has does not interfere with normal testicular descent in male mice [48]. The increased INSL3/RXFP2 signaling activity may instead reflect differences in genetic background or cellular composition of the fetal gubernaculum between strains and/or secondary effects related to impaired gubernacular development. We also observed a minimal rise in serum INSL3 in female fetuses at E17, corresponding to the temporal peak in males and occurring in both strains. Although unlikely to be biologically significant, we cannot explain this observation at present, and further studies are needed to confirm this finding.

In summary, the orl rat provides a valuable model for studies of gubernacular development and the genetic basis of cryptorchidism. Our studies suggest that localized muscle pattern abnormalities occur within the prenatal orl gubernaculum and contribute to an incompletely penetrant cryptorchidism phenotype. Although the defect targets muscle-related transcripts, these are largely not directly responsive to INSL3 or DHT in vitro, consistent with our prior conclusion that muscle-specific gene expression in the gubernaculum is not directly targeted by testicular hormones at E17 [8, 9]. The genetic basis of cryptorchidism in the orl strain remains incompletely defined but may involve synergistic targeting of muscle phenotype/behavior, ECM metabolism, and/or mechanical properties of the gubernaculum and may involve one or more loci involved in embryonic patterning. Our data suggest that one of several potential risk alleles for cryptorchidism contributes to reduced testosterone production, but we have found no evidence for a genetic defect that directly targets hormone production or response in the orl fetus. The differences in the orl transcriptome support a role for defective androgen- and upregulated INSL3-dependent signaling in the orl fetus, although these differences may simply reflect developmental delays. Further studies are needed to identify the genetic variants, pathways, and mechanisms that contribute to abnormal development and malfunction of the gubernaculum in the orl strain.

REFERENCES

1. Husmann DA, McPhaul MJ. Time-specific androgen blockade with flutamide inhibits testicular descent in the rat. Endocrinology 1991; 129: 1409–1416.
2. Spencer JR, Torrado T, Sanchez RS, Vaughan ED Jr, Imperato-McGinley J. Effects of flutamide and finasteride on rat testicular descent. Endocrinology 1991; 129:741–748.
3. Welsh M, Saunders PT, Fisken M, Scott HM, Hutchison GR, Smith LB, Sharpe RM. Identification in rats of a programming window for reproductive tract masculinization, disruption of which leads to hypospadias and cryptorchidism. J Clin Invest 2008; 118:1479–1490.
4. Barteczko KJ, Jacob MI. The testicular descent in human. Origin, development and fate of the gubernaculum Hunteri, processus vaginalis peritonei, and gonadal ligaments. Adv Anat Embryol Cell Biol 2000; 156: III–X.
5. Heyns CF. The gubernaculum during testicular descent in the human fetus. J Anat 1987; 153:93–112.
6. Kaftanovskaya EM, Huang Z, Barbara AM, De Gendt K, Verhoeven G, Gorlov IP, Agoulnik AI. Cryptorchidism in mice with an androgen receptor ablation in gubernaculum testis. Mol Endocrinol 2012; 26: 598–607.
7. Kaftanovskaya EM, Feng S, Huang Z, Tan Y, Barbara AM, Kaur S, Truong A, Gorlov IP, Agoulnik AI. Suppression of insulin-like 3 receptor reveals the role of beta-catenin and Notch signaling in gubernaculum development. Mol Endocrinol 2011; 25:170–183.
8. Barthold JS, Wang Y, Robbins A, Pike J, McDowell E, Johnson KJ, McCahan SM. Transcriptome analysis of the dihydrotestosterone-exposed fetal rat gubernaculum identifies common androgen and insulin-like 3 targets. Biol Reprod 2013; 89:143.
9. Johnson KJ, Robbins AK, Wang Y, McCahan SM, Chacko JK, Barthold JS. Insulin-like 3 exposure of the fetal rat gubernaculum modulates expression of genes involved in neural pathways. Biol Reprod 2010; 83: 774–782.
10. Barthold JS, Si X, Stabley D, Sol-Church K, Campion L, McCahan SM. Failure of shortening and inversion of the perinatal gubernaculum in the cryptorchid long-evans orl rat. J Urol 2006; 176:1612–1617.
11. Barthold JS, McCahan SM, Singh AV, Knudsen TB, Si X, Campion L, Akins RE. Altered expression of muscle- and cytoskeleton-related genes in a rat strain with inherited cryptorchidism. J Androl 2008; 29:352–366.
12. Anand-Ivell R, Heng K, Hafen B, Setchell B, Ivell R. Dynamics of INSL3 peptide expression in the rodent testis. Biol Reprod 2009; 81:480–487.
13. Rat Genome Database Web Site, Medical College of Wisconsin, Milwaukee, WI. http://rgd.mcw.edu/. Accessed December 3, 2013.
14. Wu Z, Irizarry R, Gentleman R, Martinez-Murillo F, Spencer F. A model-based background adjustment for oligonucleotide expression arrays. J Am Stat Assoc 2004; 99:909–917.
15. Smyth GK. Linear models and empirical bayes methods for assessing differential expression in microarray experiments. Stat Appl Genet Mol Biol 2004; 3:Article3.
16. Ahnfelt-Ronne J, Jorgensen MC, Hald J, Madsen OD, Serup P, Heckscher-Sorensen J. An improved method for three-dimensional reconstruction of protein expression patterns in intact mouse and chicken embryos and organs. J Histochem Cytochem 2007; 55:925–930.
17. Dent JA, Polson AG, Klymkowsky MW. A whole-mount immunocytochemical analysis of the expression of the intermediate filament protein vimentin in Xenopus. Development 1989; 105:61–74.
18. Nation TR, Buraundi S, Farmer PJ, Balic A, Newgreen D, Southwell BR, Hutson JM. Development of the gubernaculum during testicular descent in the rat. Anat Rec (Hoboken) 2011; 294:1249–1260.
19. Bay K, Main KM, Toppari J, Skakkebaek NE. Testicular descent: INSL3, testosterone, genes and the intrauterine milieu. Nat Rev Urol 2011; 8: 187–196.
20. Spencer JR, Vaughan ED Jr, Imperato-McGinley J. Studies of the hormonal control of postnatal testicular descent in the rat. J Urol 1993; 149:618–623.
21. Benjamin DR, Juul S, Siebert JR. Congenital posterolateral diaphragmatic hernia: associated malformations. J Pediatr Surg 1988; 23:899–903.
22. Fallat ME, Hersh JH, Hutson JM. Theories on the relationship between cryptorchidism and arthrogryposis. Pediatr Surg Int 1992; 7:271–273.
23. Ferrara P, Rossodivita A, Ruggiero A, Pulitano S, Tortorolo L, Salvaggio E. Cryptorchidism associated with meningomyelocele. J Paediatr Child Health 1998; 34:44–46.
24. Koivusalo A, Taskinen S, Rintala RJ. Cryptorchidism in boys with congenital abdominal wall defects. Pediatr Surg Int 1998; 13:143–145.
25. Rundle JS, Primrose DA, Carachi R. Cryptorchism in cerebral palsy. Br J Urol 1982; 54:170–171.
26. Iizuka-Kogo A, Ishidao T, Akiyama T, Senda T. Abnormal development of urogenital organs in Dlgh1-deficient mice. Development 2007; 134: 1799–1807.
27. Mahoney ZX, Sammut B, Xavier RJ, Cunningham J, Go G, Brim KL, Stappenbeck TS, Miner JH, Swat W. Discs-large homolog 1 regulates smooth muscle orientation in the mouse ureter. Proc Natl Acad Sci U S A 2006; 103:19872–19877.
28. Chawengsaksophak K, Svingen T, Ng ET, Epp T, Spiller CM, Clark C, Cooper H, Koopman P. Loss of Wnt5a disrupts primordial germ cell migration and male sexual development in mice. Biol Reprod 2012; 86: 1–12.
29. Nagraj S, Seah GJ, Farmer PJ, Davies B, Southwell B, Lewis AG, Hutson

Article 41

JM. The development and anatomy of the gubernaculum in Hoxa11 knockout mice. J Pediatr Surg 2011; 46:387–392.

30. Rijli FM, Matyas R, Pellegrini M, Dierich A, Gruss P, Dolle P, Chambon P. Cryptorchidism and homeotic transformations of spinal nerves and vertebrae in Hoxa-10 mutant mice. Proc Natl Acad Sci U S A 1995; 92: 8185–8189.

31. Radhakrishnan J, Morikawa Y, Donahoe PK, Hendren WH. Observations on the gubernaculum during descent of the testis. Invest Urol 1979; 16: 365–368.

32. Heyns CF, Human HJ, Werely CJ, De Klerk DP. The glycosaminoglycans of the gubernaculum during testicular descent in the fetus. J Urol 1990; 143:612–617.

33. Kikuchi A, Yamamoto H, Sato A, Matsumoto S. New insights into the mechanism of Wnt signaling pathway activation. Int Rev Cell Mol Biol 2011; 291:21–71.

34. Hacker U, Nybakken K, Perrimon N. Heparan sulphate proteoglycans: the sweet side of development. Nat Rev Mol Cell Biol 2005; 6:530–541.

35. Wong K, Park HT, Wu JY, Rao Y. Slit proteins: molecular guidance cues for cells ranging from neurons to leukocytes. Curr Opin Genet Dev 2002; 12:583–591.

36. Rozario T, DeSimone DW. The extracellular matrix in development and morphogenesis: a dynamic view. Dev Biol 2010; 341:126–140.

37. Haavisto T, Nurmela K, Pohjanvirta R, Huuskonen H, El-Gehani F, Paranko J. Prenatal testosterone and luteinizing hormone levels in male rats exposed during pregnancy to 2,3,7,8-tetrachlorodibenzo-p-dioxin and diethylstilbestrol. Mol Cell Endocrinol 2001; 178:169–179.

38. vom Saal FS. Sexual differentiation in litter-bearing mammals: influence of sex of adjacent fetuses in utero. J Anim Sci 1989; 67:1824–1840.

39. Howdeshell KL, Furr J, Lambright CR, Rider CV, Wilson VS, Gray LE Jr. Cumulative effects of dibutyl phthalate and diethylhexyl phthalate on male rat reproductive tract development: altered fetal steroid hormones and genes. Toxicol Sci 2007; 99:190–202.

40. Dickinson RE, Duncan WC. The SLIT-ROBO pathway: a regulator of cell function with implications for the reproductive system. Reproduction 2010; 139:697–704.

41. Piper M, Little M. Movement through Slits: cellular migration via the Slit family. Bioessays 2003; 25:32–38.

42. Zhang B, Xiao W, Qiu H, Zhang F, Moniz HA, Jaworski A, Condac E, Gutierrez-Sanchez G, Heiss C, Clugston RD, Azadi P, Greer JJ, et al. Heparan sulfate deficiency disrupts developmental angiogenesis and causes congenital diaphragmatic hernia. J Clin Invest 2014; 124:209–221.

43. Liu J, Zhang L, Wang D, Shen H, Jiang M, Mei P, Hayden PS, Sedor JR, Hu H. Congenital diaphragmatic hernia, kidney agenesis and cardiac defects associated with Slit3-deficiency in mice. Mech Dev 2003; 120: 1059–1070.

44. Beck TF, Shchelochkov OA, Yu Z, Kim BJ, Hernandez-Garcia A, Zaveri HP, Bishop C, Overbeek PA, Stockton DW, Justice MJ, Scott DA. Novel frem1-related mouse phenotypes and evidence of genetic interactions with gata4 and slit3. PLoS One 2013; 8:e58830.

45. Slavotinek AM, Tifft CJ. Fraser syndrome and cryptophthalmos: review of the diagnostic criteria and evidence for phenotypic modules in complex malformation syndromes. J Med Genet 2002; 39:623–633.

46. Kramer SG, Kidd T, Simpson JH, Goodman CS. Switching repulsion to attraction: changing responses to slit during transition in mesoderm migration. Science 2001; 292:737–740.

47. Huang Z, Rivas B, Agoulnik AI. Insulin-like 3 signaling is important for testicular descent but dispensable for spermatogenesis and germ cell survival in adult mice. Biol Reprod 2012; 87:143.

48. Adham IM, Steding G, Thamm T, Bullesbach EE, Schwabe C, Paprotta I, Engel W. The overexpression of the insl3 in female mice causes descent of the ovaries. Mol Endocrinol 2002; 16:244–252.